Acta Crystallographica Section D
Biological Crystallography
ISSN 0907-4449

Understanding the role of Leu22 variants in methotrexate resistance: comparison of wild-type and Leu22Arg variant mouse and human dihydrofolate reductase ternary crystal complexes with methotrexate and NADPH

Vivian Cody,* Joe R. Luft and Walt Pangborn

Hauptman–Woodward Medical Research Institute, 73 High Street, Buffalo, NY 14203, USA

Correspondence e-mail: cody@hwi.buffalo.edu

Received 16 September 2004
Accepted 22 November 2004

PDB References: L22R mDHFR, 1u70, r1u70sf; L22R hDHFR, 1u71, r1u71sf; L22 mDHFR, 1u72, r1u72sf.

Structural data are reported to 2.5 Å resolution for the first full analysis of the methotrexate-resistant Leu22Arg (L22R) variant of mouse dihydrofolate reductase (mDHFR) crystallized as a ternary complex with methotrexate (MTX) and the cofactor NADPH. These results are compared with the MTX and NADPH ternary complexes of L22R human DHFR (hDHFR) and those of mouse and human wild-type DHFR enzymes. The conformation of mDHFR Arg22 is such that it makes hydrogen-bonding contacts with Asp21, Trp24 and a structural water molecule, observations which were not made in the L22R hDHFR ternary complex. These data show that there is little difference between the structures of the wild type and L22R variant for either mouse or human DHFR; however, there are significant differences between the species. Comparison of these structures reveals that the active site of mDHFR is larger than that in the hDHFR structure. In mDHFR, the position of MTX is shifted 0.6 Å toward helix *C* (residues 59–65), which in turn is shifted 1.2 Å away from the active site relative to that observed in the hDHFR ternary complexes. In the L22R variant mDHFR structure, MTX makes shorter contacts to the conserved residues Ile7, Val115 and Tyr121 than in the L22R variant human DHFR structure. These contacts are comparable in both wild-type enzymes. The unexpected results from this comparison of the mouse and human DHFR complexes bound with the same ligand and cofactor illustrate the importance of detailed study of several species of enzyme, even when there is a high sequence homology between them. These data suggest that the differences in binding interactions of the L22R variant are in agreement with the weaker binding affinity for MTX in the variant enzymes; the larger size of the binding site in mDHFR supports the observation that the binding affinity of MTX for L22R mDHFR is significantly weaker than that of the L22R hDHFR enzyme.

1. Introduction

Dihydrofolate reductase (DHFR) catalyzes the reduction of folic acid to dihydrofolic acid and to tetrahydrofolic acid, an essential cofactor in the biosynthesis of thymidylate, purines and glycine. The folic acid analogue methotrexate (MTX) has been shown to bind tightly to the active site of the enzyme, resulting in the death of exposed cells (Blakley, 1995). Although MTX has been widely used as a chemotherapeutic agent for the treatment of many cancers, its lack of specificity for tumor cells and its high toxicity profile for many types of cancer hamper its effectiveness (Schweitzer *et al.*, 1990).

© 2005 International Union of Crystallography
Printed in Denmark – all rights reserved

```
      1                          22                                  50
MOUSE MVRPLNCIVA VSQNMGIGKN GDRPWPPLRN EFKYFQRMTT TSSVEGKQNL
HUMAN MVGSLNCIVA VSQNMGIGKN GDRPWPPLRN EFRYFQRMTT TSSVEGKQNL
      51                                                     100
MOUSE VIMGRKTWFS IPEKNRPLKD RINIVLSREL KEPPRGAHFL AKSLDDALRL
HUMAN VIMGKKTWFS IPEKNRPLKG RINLVLSREL KEPPQGAHFL SRSLDDALKL
      101                                                    150
MOUSE IEQPELASKV DMVWIVGGSS VYQEAMNQPG HLRLFVTRIM QEFESDTFFP
HUMAN TEQPELANKV DMVWIVGGSS VYKEAMNHPG HLKLFVTRIM QDFESDTFFP
      151                                 186
MOUSE EIDLGKYKLL PEYPGVLSEV QEEKGIKYKF EVYEKKD
HUMAN EIDLEKYKLL PEYPGVLSDV QEEKGIKYKF EVYEKND
```

Figure 1
Sequence comparison for mouse and human dihydrofolate reductase (changes between sequences are highlighted in bold and coloured red for mouse and cyan for human). The mutation at position 22 is underlined and shown in violet.

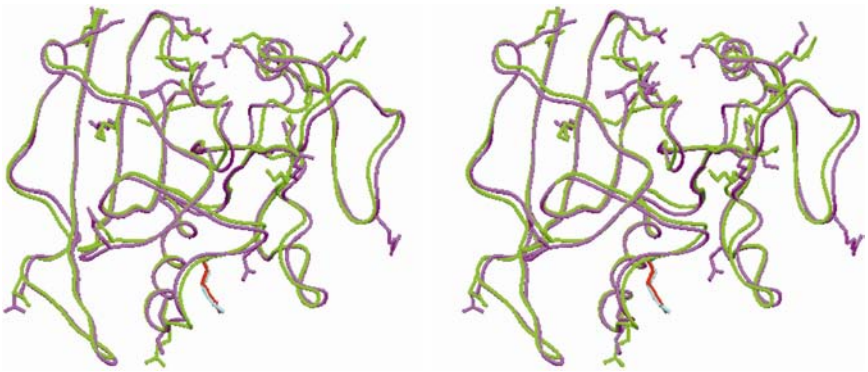

Figure 2
Comparison of the backbone of mouse (violet) and human (green) DHFR highlighting the distribution of the 19 residue changes between the sequences of the two enzymes (Table 1). 16 of these changes occur on the surface of the enzyme and none occur in the substrate-binding site. Position Arg22 is shown in cyan. The drawing was made with *SETOR* (Evans, 1993).

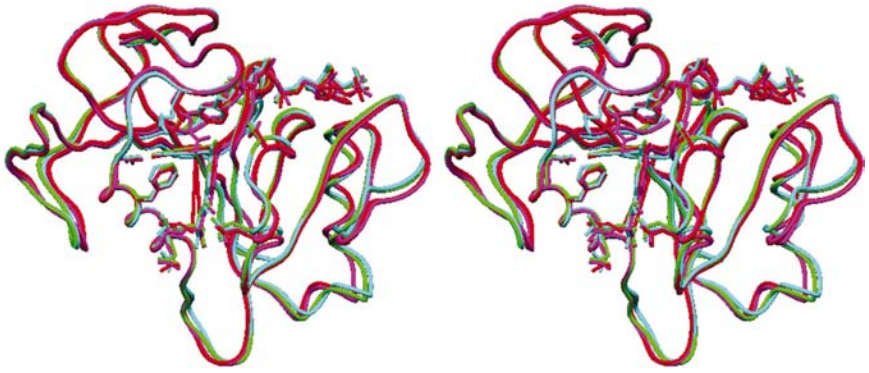

Figure 3
Superposition of the MTX–NADPH ternary DHFR complexes of L22R mDHFR (violet), L22R hDHFR (cyan), wild-type mDHFR (red) and wild-type hDHFR (green). Note the conformational changes in flexible loop regions. Residues Leu/Arg22, Glu30, Phe31, Gln35, Ser59 and Asn64 are shown. Drawings were made with *SETOR* (Evans, 1993).

Additionally, the development of drug resistance is also a limitation to MTX use. Resistance can be natural or acquired after drug exposure (Schweitzer *et al.*, 1990; Banerjee *et al.*, 1995). Among the mechanisms that give rise to drug resistance is a mutation in the *dhfr* gene that weakens MTX binding to DHFR. Some colon cancer cell lines that are MTX-resistant have been shown to have an altered DHFR enzyme (Srimatkandada *et al.*, 1989; Blakley *et al.*, 1993; Chunduru *et al.*, 1994; Lewis *et al.*, 1995; Ericikan-Abali, Mineishi *et al.*, 1996; Erickan-Abali, Waltham *et al.*, 1996). Four such mutations have been reported for rodent cell lines and one for a human colon cancer cell line (*i.e.* Leu22Arg/Phe and Phe31Ser/Trp; Haber *et al.*, 1981; Simonsen & Levinson, 1983; Srimatkandada *et al.*, 1989; Blakley *et al.*, 1993; Chunduru *et al.*, 1994; Lewis *et al.*, 1995).

Site-directed mutagenesis has been used to generate variants of recombinant mouse and human DHFR in order to test the role of specific amino acids in affecting the binding affinity of MTX. These studies, in particular those involving the variants Phe31Ser and Leu22Arg, revealed that these mutants showed the lowest affinity for binding of MTX (Chunduru *et al.*, 1994; Lewis *et al.*, 1995; Ericikan-Abali, Mineishi *et al.*, 1996; Erickan-Abali, Waltham *et al.*, 1996; Thillet *et al.*, 1988, 1990; McIvor & Simonsen, 1990; Morris & McIvor, 1994; Evenson *et al.*, 1996; Wagner *et al.*, 1995). Kinetic and biochemical activity data showed that although mouse and human DHFR are highly homologous (Figs. 1 and 2), the substitution of Arg for Leu22 in mDHFR decreases the affinity for MTX 30 700 times, whereas the same substitution in hDHFR decreases the affinity for MTX by only 1300 times (Mareya *et al.*, 1998). Similarly, the mDHFR L22R variant has also been shown to have low catalytic efficiency (Thillet *et al.*, 1988, 1990; Morris & McIvor, 1994). The L22R variant of mDHFR has poor catalytic properties for conferring resistance, primarily owing to the large decrease in k_{cat}. The half-life of the L22R variant of mDHFR is considerably longer than

that of wt mDHFR, as was also observed for the human variants. Kinetic data for mouse DHFR (Thillet *et al.*, 1990) showed that (i) two native enzyme conformers, E1 and E2, bind ligands with varying affinities, although only E1 can support catalysis in the forward direction, (ii) tetrahydrofolate dissociation is the rate-limiting step under steady-state turnover at low pH and (iii) the pH-dependent rate of hydride transfer from NADPH to dihydrofolate is fast and favorable.

Variants of mammalian DHFR that are insensitive to MTX have clinical relevance as they offer potential as therapeutic agents for retroviral introduction of MTX-resistance into bone-marrow stem cells (Patel *et al.*, 1997; Allay *et al.*, 1997; Blakley & Sorrentino, 1998). Relative protection from MTX was conferred by variants of mDHFR on human lymphoid cell lines (CCRF-CEM), in particular the Leu22Arg mutant (Thillet *et al.*, 1988; Patel *et al.*, 1997; Blakley & Sorrentino, 1998). The altered gene that produces L22R mDHFR can be employed as a dominant selectable marker in cultured cells expressing normal levels of wild-type DHFR (Simonsen & Levinson, 1983). Kinetic data for a series of Leu22 mutants of mDHFR showed the Arg22 variant provided the highest protection from MTX (K_i values for MTX for wild-type human and mouse DHFR are 0.0034 and 0.0075 n*M*, respectively, and for L22R human and mouse DHFR are 4.56 and 230 n*M*, respectively; Mareya *et al.*, 1998; Pineda *et al.*, 2003). Furthermore, variant DHFRs that are resistant to MTX while still maintaining sufficient catalytic activity have been shown to protect experimental animals from MTX toxicity (McIvor, 2002).

The crystal structure of mouse L1210 DHFR was first reported as the ternary complex with wild-type mDHFR and MTX and NADPH (Stammers *et al.*, 1987) and as the Glu30Asp variant mDHFR with trimethoprim (Groom *et al.*, 1991). These data (for which no coordinates were published) revealed similar interactions with mDHFR as reported for the hDHFR MTXT–NADPH complexes (Cody, Luft *et al.*, 1993; Cody, Wojtczak *et al.*, 1993). Crystallization of the MTX ternary complex with mDHFR was first carried out by soaking experiments based on the crystals of the trimethoprim–NADPH–mDHFR ternary complex (Stammers *et al.*, 1987; Groom *et al.*, 1991).

Mouse DHFR has been used as a model to test hypotheses concerning the toxic effects of MTX and to understand the mechanism of drug resistance. In order to understand the basis for differences in MTX-resistance between mouse and human DHFR, we report the first structural details for the L22R variant of mouse DHFR in complex with MTX and NADPH and for the wild-type hDHFR complex; these results are compared with those reported previously for the wild-type mDHFR ternary complex (Stammers *et al.*, 1987) and for the L22R human DHFR complex (Lewis *et al.*, 1995).

Table 1
Crystal properties and refinement statistics for mouse and human DHFR.

	L22R mDHFR	L22R mDHFR†	L22R hDHFR‡	L22 hDHFR	L22 mDHFR†
PDB code	1u70		1u71		1u72
Complex	Ternary	Ternary	Ternary	Ternary	Ternary
Unit-cell parameters					
a (Å)	42.02	43.70	86.06	87.38	43.40
b (Å)	61.54	61.60	86.06	87.38	61.30
c (Å)	43.57	41.90	77.68	76.72	41.90
γ/β (°)	116.7	116.3	120	120	116.1
Space group	$P2_1$	$P2_1$	*R*3	*R3*	$P2_1$
Resolution range (Å)	50.0–2.50	50.0–2.50	50.0–2.20	50.0–1.90	50.0–1.65
Last shell (Å)	2.56–2.50		2.3–2.2	2.0–1.90	
R_{merge} (%)	5.5			5.8	4.9
Overall completeness (%)	97.7			87.1	90.3
Completeness (last shell) (%)	96.1		60.5	55.9	
Total No. of reflections	6963		6906	8361	
No. of reflections used	6792		6383	6203	
R factor (%)	18.3	18.3	21.1	15.9	21.3
R wt	22.5		23.6	18.2	
No. of protein atoms	1516		1505	1502	
No. of water molecules	28		69	47	
Ramachandran plot§ (%)	84.0		93.7	90.0	
B factor (protein average) (Å^2)	39.6		29.8	26.5	

† Groom (1991). ‡ Lewis *et al.* (1995). § Percentage of residues in most favored region as determined by *PROCHECK*.

2. Materials and methods

2.1. Crystallization and X-ray data collection

2.1.1. Mouse DHFR. Recombinant Leu22Arg variant mouse DHFR was cloned, isolated and purified as described by Mareya *et al.* (1998). Crystals of mouse L22R DHFR were grown using hanging-drop vapor-diffusion methods from enzyme incubated with MTX and NADPH prior to crystallization. Protein droplets contained 20% PEG 4000 in 0.1 *M* HEPES buffer pH 7.5. Data were collected at room temperature on a Rigaku R-AXIS IIc area detector for the L22R mDHFR complex. Although most of the mDHFR crystals were small and of limited quality, data were collected from the best crystal that resulted in reasonable diffraction. Data for the structure were processed with *DENZO* and scaled with *SCALEPACK* (Otwinowski & Minor, 1997). The unit-cell parameters and crystal properties are listed in Table 1 for the NADPH ternary complex with the inhibitor MTX.

2.1.2. Human DHFR. Samples of both the L22R variant and wild-type hDHFR were prepared as described by Lewis *et al.* (1995). Crystals of both enzymes were grown using hanging-drop methods from enzyme incubated with MTX and NADPH. Protein droplets contained 62% ammonium sulfate in 0.1 *M* phosphate buffer pH 7.0 for the L22R variant and 65% ammonium sulfate in 0.1 *M* phosphate buffer pH 8.0 for the wild-type enzyme.

Data were collected at room temperature on a Rigaku R-AXIS IIc area detector for all structures and data for all

Table 2
R.m.s.d.s.

	Target σ	R.m.s. σ, L22R mDHFR	R.m.s. σ, L22R hDHFR	R.m.s. σ, wt hDHFR
Distances (Å)				
Bonds	0.020	0.017	0.018	0.016
Angles	0.040	0.064	0.059	0.053
Planar 1–4	0.050	0.069	0.064	0.053
Single torsion	0.050	0.247	0.254	0.231
Planar groups	0.020	0.014	0.013	0.012
Chiral volume	0.150	0.224	0.176	0.170
Multiple torsion	0.500	0.345	0.303	0.270
Possible hydrogen bond	0.500	0.221	0.258	0.245
Torsion angles (°)				
Planar	3.0	2.7	2.5	2.1
Staggered	15.0	28.8	23.1	23.4
Orthonormal	20.0	24.6	17.0	18.3

structures were processed with *DENZO* and scaled with *SCALEPACK* (Otwinowski & Minor, 1997). The unit-cell parameters and crystal properties for these structures are listed in Table 1.

2.2. Structure determination and refinement

All structures were solved by molecular-replacement methods with *PROLSQ* (Hendrickson & Konnert, 1980; Finzel, 1987) using coordinates for hDHFR (PDB code 1mvs). In the case of the mouse DHFR data, all residues that differed from those in the human DHFR sequence (Fig. 1) were set to alanine prior to carrying out the model search. The side chains of the mouse-DHFR-specific sequences were fitted to their observed electron density. Between least-squares minimizations, the structures were manually adjusted to fit difference electron density and verified by a series of omit maps calculated from the current model with deleted fragments. Model building was carried out on a Silicon Graphics R1000 workstation using *CHAIN* (Sack, 1988). All data were refined to their resolution limits (Table 1). All structures were revealed to be ternary complexes with MTX and NADPH. There was limited electron density for the N-terminal four residues of L22R mDHFR and these were left out of the structure. The Ramachandran conformational parameters generated by *PROCHECK* (Laskowski *et al.*, 1993) for the final models from the last cycle of refinement showed that for the mDHFR and hDHFR complexes, respectively, 84 and 93% of the residues had the most favored conformation and none were in disallowed regions.

When the preliminary analysis of the L22R mDHFR complex was reported (Cody *et al.*, 2001), coordinates for the wild-type mDHFR ternary complex with MTX and NADPH were not published. However, Groom (personal communication) has now made available the coordinates for wild-type mDHFR and a second determination of the L22R mDHFR–MTX–NADPH ternary complex. Since the structure of L22R mDHFR complex from the Groom data is similar to that reported here, all comparisons are with respect to this reported structure determination. Despite the relatively poor resolution of the L22R mDHFR ternary complex reported here, these data are consistent with those reported by Groom for the same complex, which also diffracted to 2.5 Å resolution and refined to 18.3% (Table 1). Similarly, crystals of the wild-type mDHFR ternary complex with MTX and NADPH diffracted to 1.65 Å and data were refined to 20.7% (Groom, 1991). These data differ from those reported earlier (Stammers *et al.*, 1987). In the case of the L22R and wild-type hDHFR structures, the data are of reasonable quality and resolution (Table 1). Comparison of these data shows that the overall structural details of the L22R variant of mouse and human DHFR complexes are similar (Fig. 3). There are changes in the backbone conformation in flexible loop regions on the surface compared with the structure of L22R hDHFR–MTX ternary complex, arising in part from different lattice contacts (Table 2).

3. Results

3.1. Overall structure

The overall characteristics of the folds of these mouse and human DHFR enzyme complexes are similar to those previously reported (Lewis *et al.*, 1995; Stammers *et al.*, 1987; Groom *et al.*, 1991; Cody, Luft *et al.*, 1993; Cody, Wojtczak *et al.*, 1993) (Fig. 3). In the L22R variant of the mDHFR ternary complex with MTX and NADPH there are conformational differences in the range 0.4–1.5 Å between the flexible regions encompassing loop 82 (residues 80–85), loop 103 (residues 93–105) and loop 165 (residues 163–169) compared with the L22R variant of hDHFR.

3.2. L22R variant

Interpretation of the electron density around Arg22 in the mDHFR–MTX–NADPH ternary complex (Fig. 4) shows that its conformation differs from that observed in the hDHFR L22R variant MTX–NADPH ternary enzyme complex (Lewis *et al.*, 1995). Arg22 forms interactions with Asp21, Trp24 (Fig. 5*a*) and a structural water molecule (not shown). The network also includes a contact through the water molecule with Ser59 that is absent in the L22R hDHFR variant. The closest contacts made by Arg22 in the hDHFR complex involve the adjacent Asp21 side chain with the Arg22 backbone nitrogen. In the case of the L22R hDHFR variant, the alternate conformation for Arg22 permits an interaction of the Arg22 side chain with the backbone carbonyl of Trp24 and with the backbone carbonyl of Arg22 itself. These contacts are not present in the L22R mDHFR variant (Table 3).

3.3. Inhibitor binding

The interactions of the 2,4-diaminopteridine ring of MTX in all structures compared here preserve the overall pattern of contacts with invariant residues in the DHFR active site. As observed in other DHFR–inhibitor complexes (Cody *et al.*, 1999, 2003; Cody, Galitsky, Luft, Pangborn, Rosowsky *et al.*, 2002; Cody, Galitsky, Luft, Pangborn, Queener *et al.*, 2002; Volz *et al.*, 1982; Matthews *et al.*, 1985), a hydrogen-bonding

network involving structural water, the conserved residues Thr136, Glu30 and Trp24 and the N1 nitrogen and 2-amino group of MTX is maintained (Fig. 5*b*; Table 3). The pteridine ring N8 makes contact with Glu30 and Trp24 through a structural water molecule that is observed in most DHFR structures. The 4-amino group of MTX maintains its contacts with the conserved residues Ile7, Val115 and Tyr121 and with NADPH. As illustrated in Table 3, there are significant differences in the contacts involving the variant L22R mDHFR and those of the wild-type mDHFR and the variant L22R hDHFR and the wild-type hDHFR complexes.

Comparison of these data (Figs. 3 and 6) reveals that the structures of the wild-type and L22R variant DHFR are similar with few changes between pairs of the same species; however, conformational changes are observed between the mouse and human DHFR enzyme pairs. These data show that there is a shift in the position of MTX (∼0.6 Å) such that in the L22R mDHFR complex the intramolecular contacts of MTX to the conserved residues Ile7, Val115 and Tyr121 are shorter than those observed in the L22R hDHFR ternary complex (Table 3). Similarly, these contacts are similar in the wild-type mouse and human DHFR complexes.

MTX also makes a series of hydrogen-bonding contacts involving the benzoyl keto group and Asn64 and the glutamate α-carboxylate with Arg70. As illustrated (Table 3; Fig. 5*b*), the α-carboxylate of MTX makes close contacts with the side chains of Arg70 and Gln35, while the MTX *p*-aminobenzoyl keto function makes close contact with Asn64 (Fig. 5*b*). In contrast to the pteridine-ring interactions, these data show that the closest contacts to the glutamate moiety are made in the hDHFR structures. The glutamate moiety makes closer contacts to Asn64 in both the L22R variants of mouse and human DHFR than in either of the wild-type structures (Table 3).

Table 3
Inhibitor contacts in mDHFR and hDHFR ternary complexes with MTX and NADPH.

	L22R mDHFR	L22R mDHFR†	L22R hDHFR‡	L22 hDHFR	L22 mDHFR†
MTX N4···Ile7	2.78	2.66	3.55	2.72	2.68
MTX N4···Val115	2.76	2.92	3.18	3.21	3.07
MTX N4···Tyr121	3.05	3.07	4.06	3.33	3.21
MTX N2···Glu30	2.90	2.67	2.98	3.31	2.61
MTX N1···Glu30	2.96	2.79	2.93	2.93	2.98
W···Glu30	3.52	2.65	—	2.65	2.80
MTX N8···W	3.40	3.80	—	3.18	3.45
W···Trp24	2.94	3.62	—	3.86	3.30
MTX O17···Asn64	3.22	3.17	2.60	2.76	3.54
MTX Oα1···Arg70 NH1	3.10	2.72	2.97	2.66	2.75
MTX Oα2···Arg70 NH2	3.23	2.82	3.18	2.59	3.48
MTX Oα2···Gln35 N	3.01	2.93	2.85	3.29	3.17
Arg70 NH2···Lys68 O	3.09	2.67	3.30	2.63	2.93
Asp21 O···Arg22 N	3.31	3.10	2.57	2.94	3.48
Arg22 NH1···Asp21 O	2.97	3.73	4.25	—	—
Arg22 NH2···W24	—	2.76	2.41	—	—
Arg22 NH2···Arg22 O	—	—	3.38	—	—
Arg22 NH1···W	2.70	—	—	—	—
Arg22 NH2···W	3.07	—	—	—	—

† Groom (1991). ‡ Lewis *et al.* (1995).

3.4. Cofactor binding

Although the cofactor NADPH is bound in an extended conformation in all structures, similar to other cofactor complexes (Cody *et al.*, 1999, 2003; Cody, Galitsky, Luft, Pangborn, Rosowsky *et al.*, 2002; Cody, Galitsky, Luft, Pangborn, Queener *et al.*, 2002; Volz *et al.*, 1982), there is variation in the conformation of the nicotinamide-ribose and the pyrophosphate moieties, in particular for the L22R hDHFR complex (*i.e.* ξ_n and φ_n; Table 4; Fig. 7). There are also variations in the position of the phosphate O atom (O8) in the L22R mDHFR structure that give rise to conformational differences compared with the other structures. The carboxamide group of the nicotinamide ring, which is *syn* to the nicotinamide ring N, makes a series of strong hydrogen-bonding contacts with the conserved residues Ala9, Ile16, Tyr121 and the 4-amino group of MTX. These contacts are similar to those observed in other hDHFR and *Pneumocystis carinii* DHFR (pcDHFR) complexes, although the contacts to MTX are weaker than in the other structures (Cody, Galitsky, Luft, Pangborn, Rosowsky *et al.*, 2002; Cody, Galitsky, Luft, Pangborn, Queener *et al.*, 2002). The conserved *cis*-peptide between the invariant Gly116 and Gly117 permits interaction with the pyrophosphate O atoms that are positioned at the end of the central helix *C*. The largest changes in the cofactor conformation also occur at this position (Table 4; Fig. 7). The pyrophosphate O atoms make a series of close contacts with the backbone N atoms of Lys55, Gly117 and Ser118.

3.5. Subdomain movement

To understand how the structures of mouse and human DHFR complexes differ in detail, a least-squares fit of the two enzymes was made by superimposing sequences Glu30–Gln35 and Ser59–Arg70 (Fig. 3). Comparison of mouse and human L22R variant DHFR structures shows that the position of MTX in the L22R mDHFR complex is shifted (∼0.6 Å) with respect to that observed in the L22R hDHFR complex (Fig. 6). There is also a shift of 1.2–1.5 Å in the position of helix *C* (residues 59–65) for the L22R mDHFR complex compared with the L22R hDHFR complex. These shifts are also noted between the wild-type mouse and human DHFR structures and thus they are not influenced by the L22R variant substitution. Similar shifts in helix *C* have been observed in other DHFR structures, in particular pcDHFR complexes (Cody *et al.*, 1999; Cody, Galitsky, Luft, Pangborn, Rosowsky *et al.*, 2002; Cody, Galitsky, Luft, Pangborn, Queener *et al.*, 2002; Volz *et al.*, 1982; Matthews *et al.*, 1985; Sawaya & Kraut, 1997).

3.6. Active-site size

The overall size of the mouse DHFR ligand-binding cavity is larger than that of the hDHFR structures, as reflected in the distances between C^{α} positions across the ligand-binding cavity. For example, the distance between Glu30 and Ser59 is 16.9 and 16.2 Å for the wild-type mouse and wild-type human DHFR structures, respectively. These values are 16.4 and

15.3 Å, respectively, for the mouse and human L22R variants. The distance between the C^{α} of Leu22 and Glu30 is 12.2 and 12.0 Å, respectively, for wild-type mouse and human DHFR, while in the L22R variants these values are 12.2 and 13.8 Å, respectively. Similarly, the closest contacts of Leu22 to MTX are ∼5 Å for the wild-type mouse and human DHFR structures, respectively, but increase to 5–7 Å in the L22R variants, respectively. The closest contact of the cofactor nicotinamide ring to MTX is 3.1 Å (Nic C4···N5 MTX) in the wild-type mDHFR complex, but is 3.4 Å in the wild-type hDHFR structure. These contacts are 3.4 and 3.7 Å, respectively, for the L22R mouse and human DHFR complexes. In summary, these variations reflect innate differences between the mouse and human enzymes.

4. Discussion

These crystallographic studies provide the first report of the MTX-resistant variant L22R of mouse DHFR and describe for the first time detailed structural comparisons between the wild-type and L22R variant mouse and human DHFR ternary complexes with MTX and NADPH. These data reveal that (i) Arg22 interacts with Asp21 and Trp24, (ii) mDHFR Arg22 has a different conformation to that in the L22R hDHFR complex, (iii) the position of MTX is shifted relative to that observed for the L22R hDHFR–MTX–NADPH complex, (iv) there is a conformational shift in helix *C* and (v) there are several changes in the flexible loop regions of the cofactor subdomain between the two species of enzyme.

Access to the coordinates for the wild-type mDHFR–MTX–NADPH ternary complex (and a second data set for the L22R mDHFR ternary complex; Groom, personal communication) provided the first opportunity to make a detailed comparison between like pairs of wild-type and L22R complexes for mouse and human DHFR. The unexpected observation from these data is that the structures of the wild type and L22R variant are similar to each other in the same species, but not between species. There are significant differences between the mouse and human DHFR structural pairs that result in the active-site cavity being larger in the mouse DHFR structures. There is also a subdomain shift of helix *C* in the mDHFR complexes that further enlarges the active-site volume compared with the hDHFR structures that is independent of the variant substitution pattern. Another correlation is that in the mDHFR complexes the pteridine ring of MTX binds more tightly to the conserved residues Ile7, Val115 and Tyr121 than in the hDHFR complexes. This is in contrast to the shorter contacts in the hDHFR complexes made between the *p*-aminobenzoylglutamate moiety of MTX and residues Asn64 and Arg70. Additionally, the backbone carbonyl of Lys68 makes closer contacts with the side chain of Arg70 in the wild-type human and mouse DHFR structures than in the L22R mutants of both human and mouse enzymes.

The structural data for the wild-type mDHFR complex differ from those originally reported (Stammers *et al.*, 1987) for the soaked complexes, in contrast to the co-crystallized

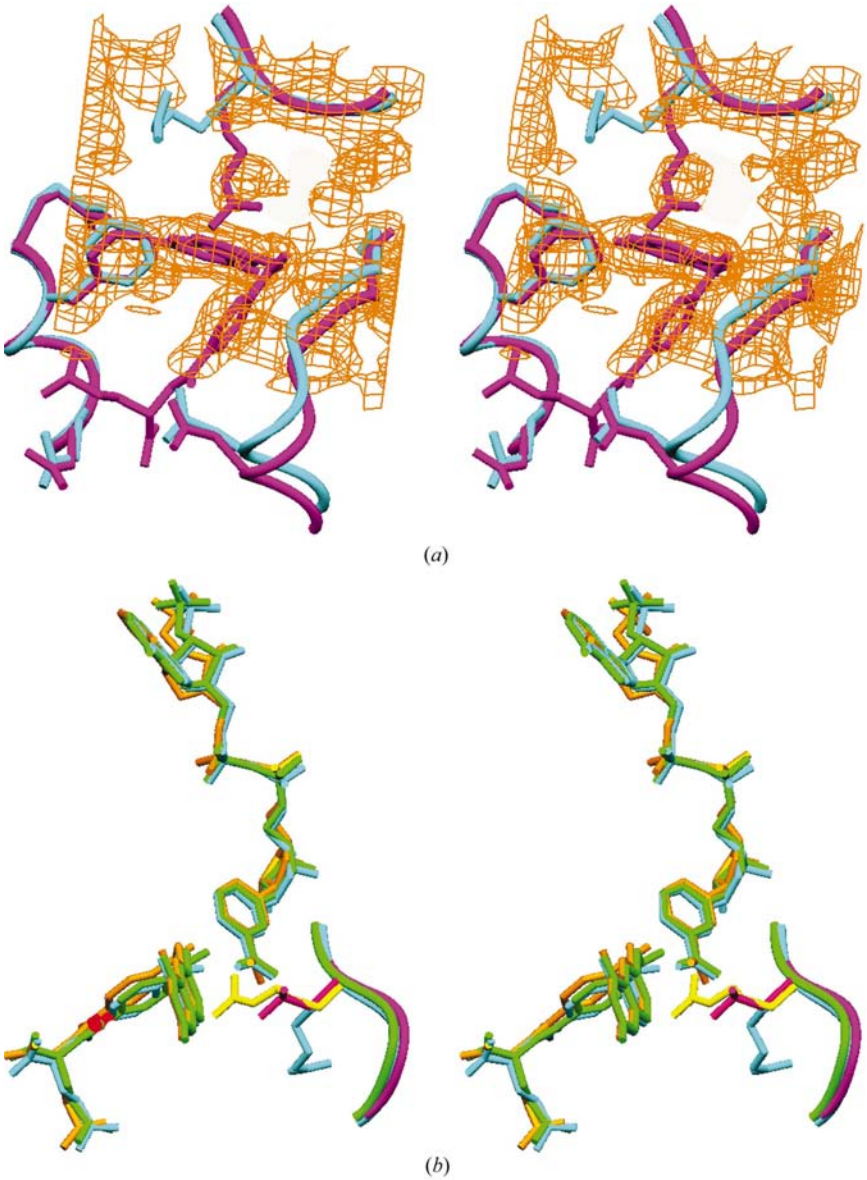

Figure 4
(*a*) Stereoview of the MTX–NADPH ternary complex for L22R mDHFR (violet), showing the conformation of Arg22. The electron density (gold) is from a $2F_o - F_c$ map for the L22R mDHFR–MTX–NADPH complex contoured at 0.8σ. Superimposed is the conformation of the L22R hDHFR–MTX–NADPH ternary complex (cyan). Also shown are the side chains of Glu30, Phe31, Gln35, Ser59 and Asn64. (*b*) Stereoview of the active site of the MTX–NADPH ternary complex with L22R mDHFR (cyan), L22R hDHFR (green with Arg22 yellow) and wild-type hDHFR (violet) with Leu22 (red). MTX and NADPH are also shown.

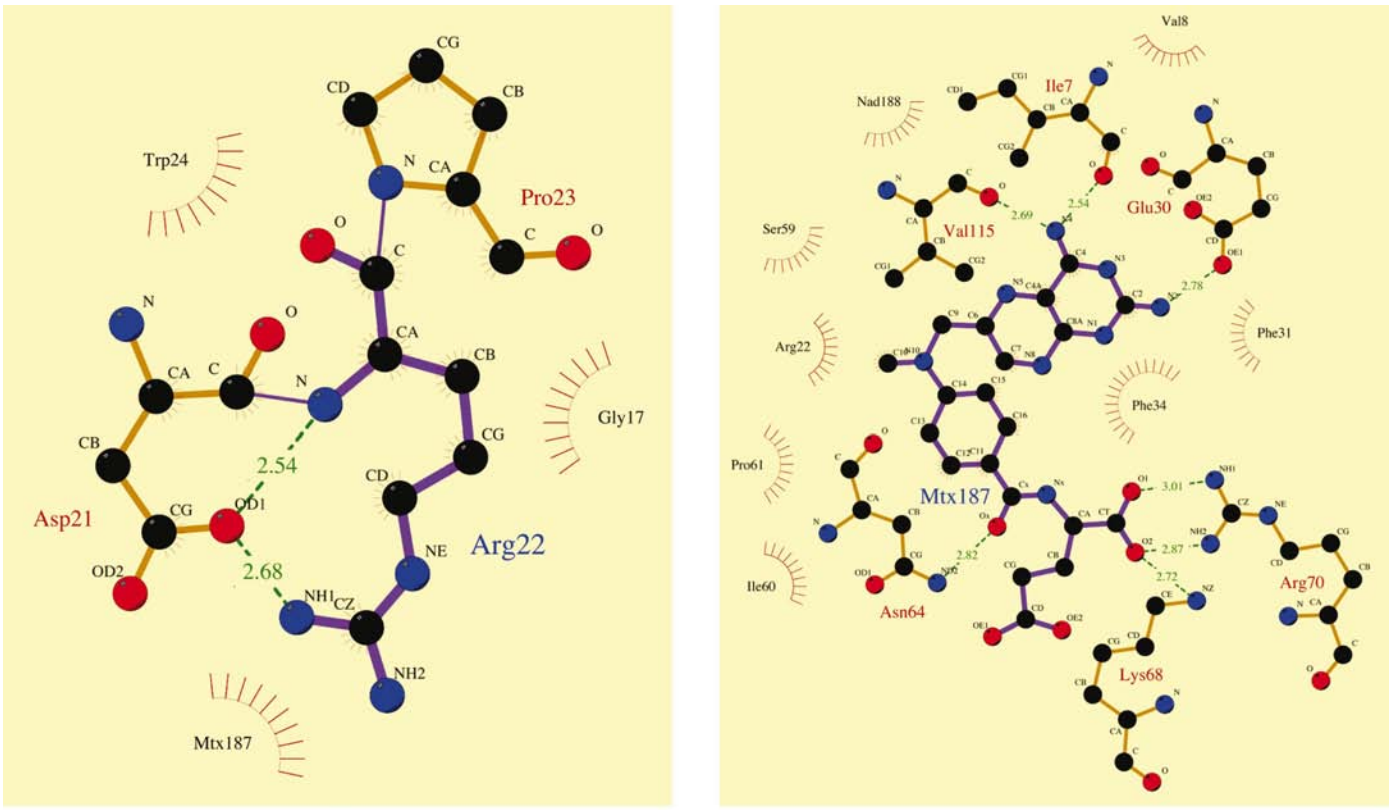

Figure 5
(*a*) View of the Arg22 contacts for L22R mDHFR. Drawn with *LIGPLOT* (Wallace *et al.*, 1995). (*b*) View of the contacts to MTX for L22R mDHFR–MTX–NADPH complex. Note: Glu30 makes a hydrogen-bonding contact to MTX N1 and N2 that is not shown in this projection. Drawn with *LIGPLOT* (Wallace *et al.*, 1995).

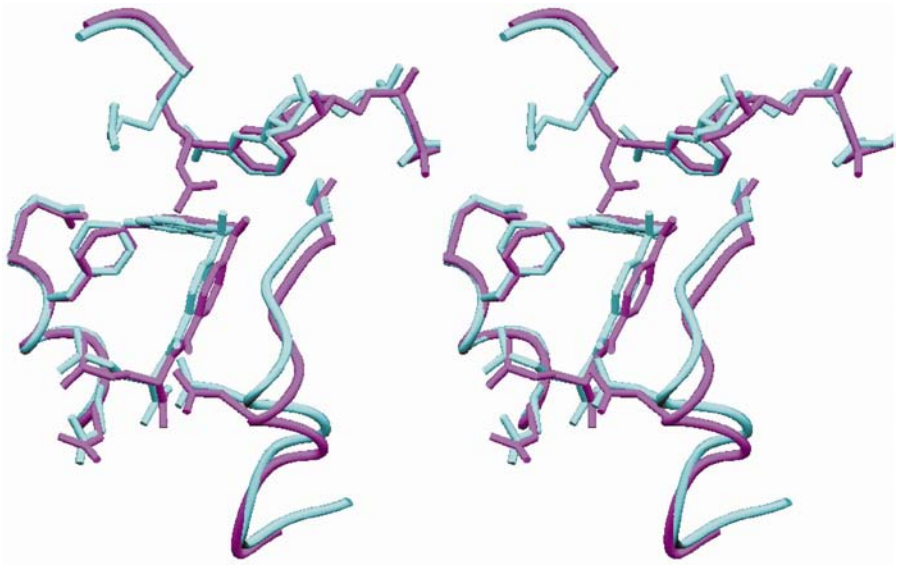

Figure 6
Stereoview of the active site for MTX–NADPH ternary complexes with L22R mDHFR (violet) and L22R hDHFR (cyan). Side chains are shown for Arg22, Glu30, Phe31, Gln35, Ser59 and Asn64. Note the shift in helix *C* and the differences in the conformation of Arg22.

experiments that were made available here (Groom, 1991). In this determination (Groom, 1991), the contacts of the MTX α-carboxylate are maintained with Arg70 and the conformation of Phe31 is similar to that reported for the hDHFR structures here. It is now recognized that when there is a *p*-aminobenzoylglutamate moiety present, the antifolate α-carboxylate makes a hydrogen-bond contact to the conserved Arg70. However, when the inhibitor does not occupy this part of the binding pocket there is a subdomain shift that brings the conserved Arg70 into contact with Gln35 (Cody, Wojtczak *et al.*, 1993; Cody *et al.*, 1999, 2003, Cody, Galitsky, Luft, Pangborn, Rosowsky *et al.*,. 2002; Cody, Galitsky, Luft, Pangborn, Queener *et al.*, 2002). Therefore, conformational changes that were noted in the previous report (Stammers *et al.*, 1987) and that were considered important in explaining differences in biological activity between mouse and human DHFR are not supported by the more recent data for the wild-type mDHFR complex.

Despite a high sequence homology between mouse and human DHFR (Table 1), their kinetic properties differ substantially and the mouse enzyme is more susceptible to conformational changes. As illustrated (Fig. 1), there are no sequence differences between the mouse and

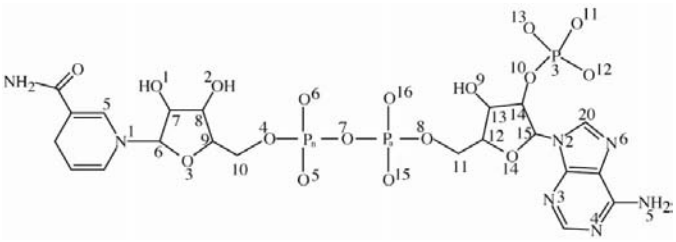

Figure 7
NADPH numbering scheme (see Table 4).

Table 4
Cofactor conformation in mouse and human DHFR ternary complexes with MTX and NADPH.

See Fig. 7 for NADPH numbering. Subscript n, torsion angles for nicotinamide nucleoside; subscript a, torsion angles for adenine nucleoside.

		L22R mDHFR	L22R mDHFR†	L22R hDHFR‡	L22 hDHFR	L22 mDHFR†
χ_n	C5—N1—C6—C7	122.5	134.5	144.5	140.3	128.8
ξ_n	C8—C9—C10—O4	−168.8	166.6	−81.2	−136.7	−178.8
θ_n	C9—C10—O4—P_n†	171.8	137.7	−136.9	171.8	128.9
ψ_n	C10—O4—P_n—O7	4.0	68.1	−18.8	−26.9	62.3
φ_n	O4—P_n—O7—P_a†	121.6	91.8	93.4	114.0	68.8
φ_a	P_n—O7—P_a—O8	79.4	139.7	157.0	138.0	160.5
ψ_a	O7—P_a—O8—C11	62.0	−72.4	−85.1	−92.9	−67.3
θ_a	P_a—O8—C11—C12	107.8	−152.6	−148.1	−146.2	−151.4
ξ_a	O8—C11—C12—C13	119.8	−178.8	−176.8	−166.8	178.0
χ_a	C14—C15—N2—C20	−111.9	−98.5	−101.1	−102.3	−102.6
θ'_a	C15—C14—O10—P3	−166.6	152.0	154.1	151.6	167.0

† Groom (1991). ‡ Lewis *et al.* (1995).

human enzyme in the ligand-binding region and the majority of the sequence changes are conservative and are found near surface loops. Thus, an explanation for the large differences between their kinetic or biological properties is not evident from the location of these sequence changes.

As noted, the L22R variant for mDHFR has the highest inhibition constant for MTX of the L22 variants tested (K_i of 4.56 n*M* compared with 230 n*M* for L22R hDHFR; Mareya *et al.*, 1998). There is a 30 700-fold decrease in MTX affinity between wild type and L22R for mDHFR, compared with a decrease of 1300-fold for the human enzyme pair (Mareya *et al.*, 1998). This weaker binding affinity for the L22R variant of mDHFR is consistent with the differences in binding interactions between the mouse and human DHFR complexes. In the wild-type structure, the closest contact of Leu22 is 4.0 Å to the C6/C7 bond of MTX, while in the L22R variant this distance is greater (>5 Å). Thus, Arg22 makes little contact with the inhibitor.

These results support the need to study several members of enzyme families even when there is a high sequence homology between members. Differences in the kinetic properties of such closely related members of the same enzyme family can be correlated with the structural changes noted in this analysis. Thus, the changes in the structure between mouse and human wild-type DHFR contribute to the significantly weaker MTX binding affinity for the mouse enzyme.

This work was supported in part from NIH grant GM51670 (VC). The authors thank Dr R. L. Blakley for the L22R variant of mouse DHFR and Dr C. Groom for providing the coordinates for the structures of wild-type mDHFR–MTX–NADPH and L22R mDHFR–MTX–NADPH ternary complexes that were reported as part of his PhD thesis.

References

Allay, J. A., Spencer, H. T., Wilkinson, S. L., Belt, J. A., Blakley, R. L. & Sorrentino, B. P. (1997). *Blood*, **90**, 3546–3554.
Banerjee, D., Ericikan-Abali, E., Waltham, M., Schnieders, B., Hochhauser, D., Li, W. W., Fan, J., Gorlick, R., Goker, E. & Bertino, J. R. (1995). *Acta Biochim. Pol.* **42**, 457–464.
Blakley, R. L. (1995). *Adv. Enzymol.* **70**, 23–102.
Blakley, R. L., Appleman, J. R., Chunduru, S. K., Nakano, T., Lewis, W. S. & Harris, S. E. (1993). *Chemistry and Biology of Pteridines and Folates*, edited by J. E. Ayling, M. G. Nair & C. M. Baugh, pp. 473–479. New York: Plenum Press.
Blakley, R. L. & Sorrentino, B. P. (1998). *Hum. Mutat.* **11**, 259–263.
Chunduru, S. K., Cody, V., Luft, J. R., Pangborn, W., Appleman, J. R. & Blakely, R. L. (1994). *J. Biol. Chem.* **269**, 9547–9555.
Cody, V., Galitsky, N., Luft, J. R. & Pangborn, W. (2001). In *Proceedings of the American Association for Cancer Research.* Philadelphia, PA, USA: American Association for Cancer Research.
Cody, V., Galitsky, N., Luft, J. R., Pangborn, W. & Gangjee, A. (2003). *Acta Cryst.* D**59**, 654–661.
Cody, V., Galitsky, N., Luft, J. R., Pangborn, W., Queener, S. F. & Gangjee, A. (2002). *Acta Cryst.* D**58**, 1393–1399.
Cody, V., Galitsky, N., Luft, J. R., Pangborn, W., Rosowsky, A. & Queener, S. F. (2002). *Acta Cryst.* D**58**, 946–954.
Cody, V., Galitsky, N., Rak, D., Luft, J. R., Pangborn, W. & Queener, S. F. (1999). *Biochemistry*, **38**, 4303–4312.
Cody, V., Luft, J. R., Ciszak, E., Kalman, T. I. & Freisheim, J. H. (1993). *Anticancer Drug Des.* **7**, 483–491.
Cody, V., Wojtczak, A., Kalman, T. I., Freisheim, J. H. & Blakley, R. L. (1993). *Chemistry and Biology of Pteridines and Folates*, edited by J. E. Ayling, M. G. Nair & C. M. Baugh, pp. 481–486. New York: Plenum Press.
Ericikan-Abali, E., Mineishi, S., Tong, Y., Nakahara, S., Waltham, M. C., Banerjee, D., Chen, W., Sadelain, M. & Bertino, J. R. (1996). *Cancer Res.* **56**, 4142–4145.
Ericikan-Abali, E., Waltham, M. C., Dicker, A. P., Schweitzer, B. I., Gritsman, H., Banerjee, D. & Bertino, J. R. (1996). *Mol. Pharmacol.* **49**, 430–437.
Evans, S. V. (1993). *J. Mol. Graph.* **11**, 134–138.
Evenson, D. A., Adams, J., McIvor, R. S. & Wagner, C. R. (1996). *J. Med. Chem.* **39**, 1763–1766.
Finzel, B. C. (1987). *J. Appl. Cryst.* **20**, 53–55.
Groom, C. R. (1991). PhD Thesis, University of Leeds, UK.
Groom, C. R., Thillet, J., North, A. C. T., Picket, R. & Geddes, A. J. (1991). *J. Biol. Chem.* **266**, 19890–19893.
Haber, D. A., Beverley, S. M., Kiely, M. L. & Schimke, R. T. (1981). *J. Biol. Chem.* **256**, 9501–9510.
Hendrickson, W. A. & Konnert, J. H. (1980). *Computing in Crystallography*, edited by R. Diamond, S. Ramachan & K. Venkatesen, p. 13.01. Bangalore, India: Indian Academy of Sciences.
Laskowski, R. A., MacArthur, M. W., Moss, D. S. & Thornton, J. M. (1993). *J. Appl. Cryst.* **26**, 283–291.
Lewis, W. S., Cody, V., Galitsky, N., Luft, J. R., Pangborn, W., Chunduru, S. K., Spencer, H. T., Appleman, J. R. & Blakley, R. L. (1995). *J. Biol. Chem.* **270**, 5057–5064.
McIvor, R. S. (2002). *Gene Therapy of Cancer*, 2nd ed., edited by E. Lattime & S. Gerson, pp. 383–392. New York: Academic Press.

McIvor, R. S. & Simonsen, C. C. (1990). *Nucleic Acids Res.* **18**, 7025–7032.
Mareya, S. M., Sorrentino, B. P. & Blakley, R. L. (1998). *Cancer Gene Ther.* **4**, 225–235.
Matthews, D. A., Bolin, J. T., Burridge, J. M., Fileman, D. J., Volz, K. W., Kaufman, B. T., Beddell, C. R., Champness, J. N., Stammers, D. K. & Kraut, J. (1985). *J. Biol. Chem.* **260**, 381–391.
Morris, J. A. & McIvor, R. S. (1994). *Biochem. Pharmacol.* **47**, 1207–1220.
Otwinowski, Z. & Minor, W. (1997). *Methods Enzymol.* **276**, 307–326.
Patel, M., Sleep, S. E. H., Lewis, W. S., Spencer, H. T., Mareya, S. M., Sorrentino, B. P. & Blakley, R. L. (1997). *Human Gene Ther.* **8**, 2069–2077.
Pineda, P., Kanter, A., McIvor, R. S., Benkovic, S. J., Rosowsky, A. & Wagner, C. R. (2003). *J. Med. Chem.* **46**, 2816–2818.
Sack, J. S. (1988). *J. Mol. Graph.* **6**, 224–225.
Sawaya, M. R. & Kraut, J. (1997). *Biochemistry*, **36**, 586–603.
Schweitzer, B. I., Dicker, A. P. & Bertino, J. R. (1990). *FASEB J.* **4**, 2442–2452.
Simonsen, C. C. & Levinson, A. D. (1983). *Proc. Natl Acad. Sci. USA*, **80**, 2495–2499.
Srimatkandada, S., Schweitzer, B. I., Moroson, B. A., Dube, S. & Bertino, J. R. (1989). *J. Biol. Chem.* **264**, 3524–3528.
Stammers, D. K., Champness, J. N., Beddell, C. R., Dann, J. G., Elipoulos, E., Geddes, A. J., Ogg, D. & North, A. C. T. (1987). *FEBS Lett.* **218**, 178–184.
Thillet, J., Absil, J., Stone, S. R. & Pictet, R. (1988). *J. Biol. Chem.* **293**, 12500–12508.
Thillet, J., Adams, J. A. & Benkovic, S. J. (1990). *Biochemistry*, **29**, 5195–5202.
Volz, K. W., Matthews, D. A., Alden, R. A., Freer, S. T., Hansch, C., Kaufman, B. T. & Kraut, J. (1982). *J. Biol. Chem.* **257**, 2538–2536.
Wagner, C. R., Huang, Z., Singleton, S. F. & Benkovic, S. J. (1995). *Biochemistry*, **34**, 15671–15680.
Wallace, A. C., Laskowski, R. A. & Thornton, J. M. (1995). *Protein Eng.* **8**, 127–134.